Chemical Physics Letters 483 (2009) 233–240

Contents lists available at ScienceDirect

Chemical Physics Letters

journal homepage: www.elsevier.com/locate/cplett

Theoretical and quantitative structural relationships of the electrochemical and electron transfer properties of [M_x@C_{82}]@[SWCNT(5,5)-armchair-C_nH_{20}] (x = 0, 1; for x = 1: M = Ce & Gd and n = 20–300) nanostructure complexes ☆

Avat Arman Taherpour *

Chemistry Department, Faculty of Science, Islamic Azad University, P.O. Box 38135-567, Arak, Iran

ARTICLE INFO

Article history:
Received 13 July 2009
In final form 22 October 2009
Available online 25 October 2009

ABSTRACT

The relationship between the number of carbon atoms (n) of the SWCNTs as an index and the first and second free energies of electron transfer ($\Delta G_{et(n)}$, n = 1, 2), as assessed using the Rehm–Weller equation on the basis of the first and second oxidation potentials ($^{ox}E_1$ and $^{ox}E_2$) of C_{82}, Ce@C_{82} and Gd@C_{82} for the predicted supramolecular complexes, between **1**–**18** and **19**–**29** with fullerene C_{82} **(a)** and the endohedral-metallofullerenes Ce@C_{82} **(b)** and Gd@C_{82} **(c)** as [M_x@C_{82}]@[SWCNT(5,5)-armchair-C_nH_{20}] (x = 0, 1; for x = 1: M = Ce & Gd; n = 20–190) **30–47**, **48–65** and **66–83** are presented. The results were extended for [M_x@C_{82}]@[SWCNT(5,5)-armchair-C_nH_{20}] (x = 0, 1; for x = 1: M = Ce & Gd; n = 200–300 **84–94**, **95–105** and **106–116**).

1. Introduction

The synthesis of C_{60} and other fullerenes [1,2] and the isolation of higher fullerenes ranging from C_{76} to C_{96} has been achieved using chromatographic techniques [1,3–6]. Whereas C_{60} and C_{70} have unique, high-symmetry structures [1,7], theoretical calculations for fullerenes larger than C_{76} have suggested that each may exist in at least two isomeric forms [1,8]. For C_{84}, 24 isomers have been postulated [1,8], and for C_{96} calculations have yielded 196 distinct isomers [1,9]. Diederich et al. [1,10] have used liquid chromatography and ^{13}C NMR to identify two isomers of C_{78}, but previous experimental studies of other higher fullerenes [1,3] have produced ambiguous results. ^{13}C NMR was utilized to determine the structures of some principal isomers of C_{78}, C_{82} and C_{84} [1,10].

The electronic structures of all isolated-pentagon C_{82} isomers has been studied using a first-principle local-density functional approach [11]. The results indicate that the ground-state isomer with C_2 symmetry is the most abundant isomer, in agreement with the conclusion obtained by recent experimental ^{13}C nuclear magnetic resonance spectroscopy [11].

Optimized geometries and ^{13}C-NMR chemical shifts of fullerene C_{82} has been calculated by density functional theory (DFT) at the B3LYP/6–31G* level for all isolated-pentagon-rule (IPR) isomers with a non-vanishing HOMO–LUMO gap (six isomers) [12]. The calculated ^{13}C NMR spectrum of the C_2 isomer agrees well with the experimental spectrum, while the predicted spectra of other isomers differ significantly from experiment. Thus, the observed isomer of C_{82} is unambiguously assigned a C_2 symmetry [12].

One of the most fascinating and unique feature of fullerenes is that there is spherical empty space inside the carbon cage. This hollow space, ranging from 0.4 to 1.0 nm in diameter going from C_{60} to C_{240} and considering the van der Waals radius of carbon (0.17 nm), is a nanometer-scale void and the volume may be varied with the size of fullerene [13a,b].

Metallofullerenes are often characterized by their 'charge-per-metal' atom encapsulated. This description implies that the oxidation of the metal atom during metallofullerene formation drives the amount of charge transfer to the fullerene cage. Formation of endohedral-metallofullerenes is thought to involve the transfer of electrons from the encapsulated metal atoms to the surrounding fullerene cage [14–17]. Significantly, C_{82} is known to form endohedral-metallofullerenes. The possibility of a charge transfer reaction during metallofullerene formation is reasonable when considering the relatively large electron affinities of fullerene cages [14–19]. It also suggests that the electronic structure of the fullerene cage is an important parameter in the formation of metallofullerenes. The voltammetry of a series of C_{82} and C_{84} metallofullerenes was investigated by Anderson et al. in an attempt to understand metallofullerene behavior in terms of its electronic structure [14–19].

In 1991, Smalley and collaborators showed that fullerenolanthanides can be produced by laser vaporization of graphite and lanthanum oxide and subsequently extracted by toluene [19–22]. The fullerenolanthanides are new kinds of organolanthanide

☆ This paper was dedicated to Professor Curt Wentrup (The University of Queensland-Australia) by the author.

* Address: Unusual Molecules and Reactive Intermediates Group, School of Molecular and Microbial Science, Chemistry Building, The University of Queensland, Brisbane, Qld 4072, Australia. Fax: +98 861 4130649.
E-mail address: avatarman.taherpour@gmail.com.

0009-2614/$ - see front matter © 2009 Elsevier B.V. All rights reserved.
doi:10.1016/j.cplett.2009.10.075

compounds stabilized by the delocalization of the negative charges on the fullerene cages and the protection of the lanthanide metals by spherical carbon ligands. Because only microgram quantities of the materials are available, electrochemistry is useful in characterizing the fullerenolanthanides [19].

The visible-near-IR absorption spectra of $Ce@C_{82}$ and $Gd@C_{82}$ are very similar to each other and display characteristic near-IR bands due to their open-shell electronic structures. The two near-IR peaks are slightly shifted: $Ce@C_{82}$, 1015 and 1425 nm and $Gd@C_{82}$, 970 and 1400 nm. The similarities in their electronic spectra may indicate that they both have the same cage structure [19].

The first reduction potentials of $Ce@C_{82}$, and $Gd@C_{82}$ were obtained by ab initio calculations and were plotted vs. the ionization potentials of the lanthanides [19,23], the ionic radii of Ln^{3+} (six coordinate) [19,24], and the ionization potentials and electron affinities of the $Ln@C_{82}$ (Ln = Ce and Gd) [19,25]. It was found that the ionic radii of Ln^{3+} showed a clear linear relationships with the first redox potentials. It has been assumed that: (1) $Ce@C_{82}$, and $Gd@C_{82}$ have the same cage structures, (2) the oxidation states of the metals are 3+, and (3) the metal-cage distances decrease in the order Ce > Gd [19]. The first oxidation and reduction processes take place on the SOMO whose electron density is higher on the cage close to the Ln^{3+} [19,26–29]. When the metal–carbon distance becomes shorter, the electrons on the SOMO are bound to the cage more strongly because of the electrostatic interaction between the electrons and the metal. This probably makes $Gd@C_{82}$ the poorest electron donor but the strongest electron acceptor between $Ce@C_{82}$, and $Gd@C_{82}$ [19]. The first voltammograms of the pure fullerenolanthanides, $Ce@C_{82}$, and $Gd@C_{82}$ has been shown before. The oxidation state of $Ln@C_{82}$ changes from 2+ to 5- or 6- in the experiments [19]. The scan started at the resting potential (−0.20 V vs. Fc/Fc^+ couple) toward the positive potential. Two oxidation peaks at +0.05 and +1.07 V were observed by DPV (differential pulse voltammograms), and the latter was irreversible by CV (cyclic voltammetry) [19]. The first reversible oxidation potential (+0.07 V) is slightly more positive than that of ferrocene, indicating that $Ln@C_{82}$ is a good electron donor [19,30a–d].

One reversible oxidation was observed for $M@C_{82}$ by CV. The oxidation state of Ce and Gd are close to that of the lanthanum and likely 3+ [19,29]. The second oxidation remained irreversible, and the peak current intensity of the second reduction was twice that of each of the other redox peaks. Furthermore, the shape of the current voltage curve suggested a simultaneous two-electron transfer rather than an overlap of two one-electron transfers [19,29].

Nanotubes are cylindrical fullerenes. These tubes of carbon are usually only a few nanometers wide, but they can range from less than a micrometer to several millimeters in length. They often have closed ends, but can be open-ended as well. There are also cases in which the tube reduces in diameter before closing off. Their unique molecular structure results in extraordinary macroscopic properties, including high tensile strength, high electrical conductivity, high ductility, high resistance to heat and relative chemical inactivity [13b]. The structures have cylindrical and planar form that it has no exposed atoms that can be easily displaced [13b].

Nanotubes of type (n, n) are called *armchair nanotubes* because of their 'W' shape perpendicular to the tube axis. They are symmetrical along the tube axis, with a short unit cell (0.25 nm or 2.5 Å) that can be repeated along the entire section of a long nanotube. All remaining nanotubes are called *chiral nanotubes* and have longer unit cell sizes along the tube axis [26–28]. The simplest type of nanotube is a cylindrical structure that, conceptually, could be formed by folding and gluing one pair of opposite sides of a rectangular graphite sheet [22–28,31a–m]. If both ends are capped, it will have at least two pentagons and therefore be a type of fullerene. Nanotubes are large, linear fullerenes with aspect ratios as large as 103–105 [28]. The walls of such a tube could have various sizes of polygons [32a–c]. Although many nano-scale fullerene materials occur regularly in applications, controlled production of many fullerenes and nanotubes with well-defined characteristics has not occurred [22–28,31a–m]. Because of their properties, they can act as lightweight, large surface-area packing materials for gas storage and hydrocarbon fuel storage devices, nanoscale devices for molecular drug delivery and as casting structures for making nanowires and nanocapsulates. Exceptionally strong nanotubes can be used to make lightweight structural materials. Nanotubes such as '*capsulates*' can help to store and carry hydrogen and other hydrocarbon-based fuel in engines or aboard spacecraft. These important groups of carbon allotropes can be easily closed on both sides. Single-wall carbon nanotubes are among the most interesting new carbon allotropes discovered in many years [26,27].

Carbon nanotubes possess many special properties, such as an open mesoporous structure, high electrical conductivity and chemical stability, as well as extremely high mechanical strength and modulus [28,31f–j]. These properties, which not only help in the transportation of ions, but also facilitate the charging of the double layer, will confer advantageous attributes in the development of electrochemical capacitors [31k]. Single-walled carbon nanotubes have been recognized as a potential electrode material for electrochemical capacitors [31l,m].

One of the most recognized structures of nanotubes is the (5,5) tube. In the (5,5) tube, the structure can be built up by successively adjoining sections of 10 C atoms. In the infinite tube, the periodic unit cell is two such sections consisting of 20 C atoms [26]. The electronic structures and electrical properties of single-wall nanotubes can be simulated from those of a layer of graphite (graphene sheet) [31f–l,m].

In Fig. 1, the (5,5) *armchair* form is shown. Fig. 1 shows the imaginary structures C_{82} **(a)**, $Ce@C_{82}$ **(b)**, $Gd@C_{82}$ **(c)** and **1–116** as $[M_x@C_{82}]@[SWCNT(5,5)\text{-armchair-}C_nH_{20}]$ ($x = 0$, 1; for $x = 1$: M = Ce & Gd; $n = 20$–300). In experiments, nanotubes may not contain any hydrogen atoms (there is no hydrogen in the electric-arc technique) and the nanotubes can be easily closed at both ends.

The electronic structures of tubular aromatic molecules derived from the metallic (5,5) armchair SWCNT for $C_{20}H_{20}$ up to $C_{210}H_{20}$ (see Fig. 1) were reported by Zhou et al. [26]. That report considered how the electronic structures of short molecular sections of the (5,5) tube relate to, differ from, and asymptotically approach that of an infinite metallic tube [26]. Some of the structural and electronic properties were investigated, such as the ionization potential, electron affinity, Fermi energy (E_f), chemical hardness, and relative energetic stability. All of these metrics show the length periodicity seen in the frontier orbitals (FOs, i.e., HOMO–LUMO: Highest Occupied Molecular Orbital–Lowest Unoccupied Molecular Orbital) gap, in contrast to the optical 'charge transfer' transition and the static axial polarizability [26]. These (5,5) nanotubes have two types of symmetry. For nanotubes with odd identification numbers (**1–17**), the point group is D_{5d}, and for nanotubes with even identification numbers (**2–18**), the point group is D_{5h}. In that study, static and TD-DFT (Time Dependent-Density Function Theory) were used to independently optimize the structure for neutral, cationic and anionic complexes. The hybrid non-local B3LYP (Becke, three-parameter, Lee–Yang–Parr) functional was utilized [26].

Infinite length SWCNTs are π-bonded aromatic structures that can be either semi-conducting or metallic, depending upon the diameter and helical angle of SWCNTs. In a pioneering 1992 DFT calculation, Mintmire et al. predicted that the infinite length (5,5) armchair SWCNT (6.70 Å diameter) would be metallic with a very low transition temperature separating the uniform (high temperature) structure from the Peierls bond alternating (low temperature) structure [31l,33]. This specific SWCNT is the elongated tube of the C_{60}, C_{70}, etc., molecular family [26].

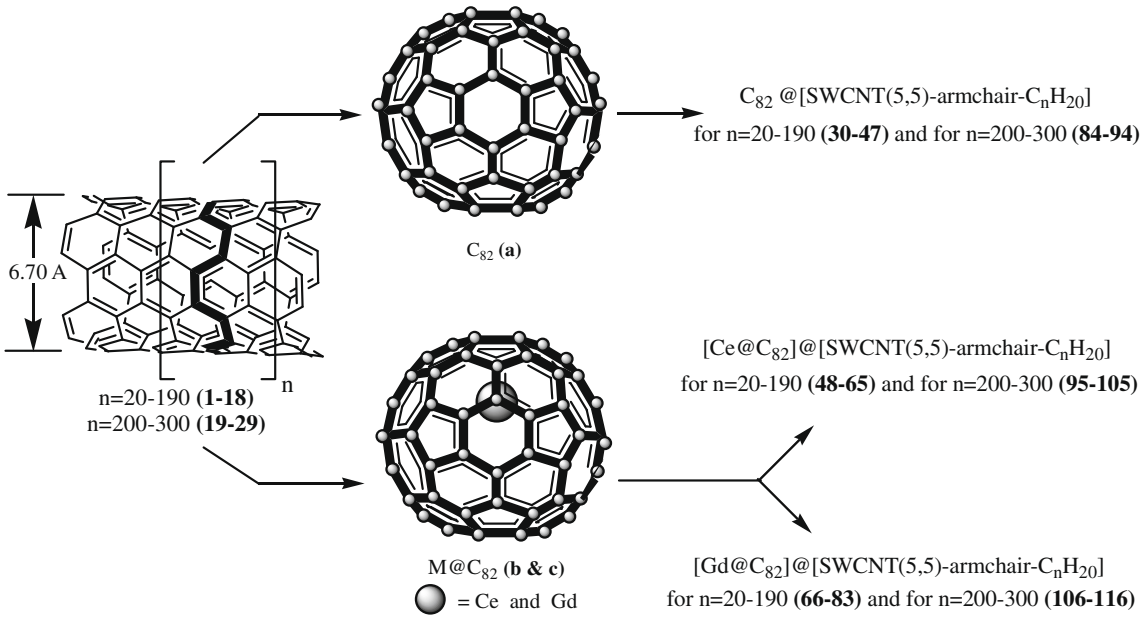

Fig. 1. The imaginary structures of C_{82} **(a)**, Ce@C_{82} **(b)**, Gd@C_{82} **(c)** and **1–116**.

Fullerene peapods are supramolecular complexes, which are formed by filling SWCNT with fullerenes from the vapor phase [34,35] Most of the previous studies are related to C_{60}@SWCNT and C_{70}@SWCNT structures [31c,36,37a–e].

The diameter sizes of C_{60} and [SWCNT(5,5)-armchair-C_nH_{20}] **1–18** were reported to be 6.70 and 6.94 Å, respectively [37b,c]. With these diameters, it is not possible to encapsulate C_{60} inside the [SWCNT(5,5)-armchair-C_nH_{20}] in the structure of C_{60}@[SWCNT (5,5)-armchair-C_nH_{20}] (see the imaginary scheme in Fig. 1).

Graph theory has been found to be a useful tool in assessing the *QSAR* (Quantitative Structure Activity Relationship) and *QSPR* (Quantitative Structure Property Relationship) [37a–e,38a–e]. Any extrapolation of results from one compound to other compounds must take into account considerations based on a Quantitative Structural Analysis Relationship Study (QSARS), which mostly depends on how close the compounds under consideration are in their physical and chemical properties [13b]. Numerous studies in the above areas have also used what are called topological indices (TI) [39a–d]. It is important to use effective mathematical methods to make strong connections between the data corresponding to several chemical properties. One of the useful numerical and structural values in unsaturated compounds like nanotubes is the degree of unsaturation (D_U). This quantity is a useful index for determining the number of cyclic structures and/or π-bonds in a molecule [37a–e,39a–d,13b]. In previous studies, a relationship between the D_U index and electron affinity, reduction potential ($^{Red}E_1$) of [SWCNT(5,5)-armchair-C_nH_{20}] as well as the free energy of electron transfer (ΔG_{et}) between [SWCNT(5,5)-armchair-C_nH_{20}] structures and fullerene C_{60} as C_{60}@[SWCNT(5,5)-armchair-C_nH_{20}] complexes was investigated [37a]. The relationship between D_U index and the free energy of electron transfer (ΔG_{et}) as assessed using the Rehm–Weller equation on the basis of the first oxidation potential ($^{ox}E_1$) of Sc_2@C_{84} and Er_2@C_{82} for the predicted supramolecular complexes between and the endohedral-metallofullerenes Sc_2@C_{84} and Er_2@C_{82} as [M_2@C*x*]@[SWCNT(5,5)-Armchair-C*n*H_{20}] (M) Er and Sc, $x = 82$ and 84) were presented and discussed before [13b].

In the study of the structural properties of π-bonds, the relationship between the number of carbon atoms of the SWCNT (C_n) index and electron affinity, reduction potential ($^{Red}E_1$) of [SWCNT(5,5)-armchair-C_nH_{20}] **1–18** (and extension the results to **19–29)** as well as the first and second free energy of electron transfer ($\Delta G_{et(n)}$, $n = 1, 2$) as assessed using the Rehm–Weller equation on the basis of the first and second oxidation potential ($^{ox}E_1$ and $^{ox}E_2$) of C_{82} **(a)** (for C_{82} just first oxidation potential ($^{ox}E_1$), Ce@C_{82} **(b)**, Gd@C_{82} **(c)** for the predicted supramolecular complexes, between **1–18**, fullerene C_{82} **(a)** and endohedral-metallofullerenes (Ce@C_{82} **(b)**, Gd@C_{82}) as [M_x@C_{82}]@[SWCNT(5,5)-armchair-C_nH_{20}] ($x = 0, 1$; for $x = 1$: M = Ce & Gd; $n = 20$–190), are presented. The results were extended for [M_x@C_{82}]@[SWCNT(5,5)-armchair-C_nH_{20}] ($x = 0, 1$; for $x = 1$: M = Ce & Gd; $n = 200$–300).

2. Graphing and mathematical methods

The number of carbon atoms of these SWCNT (C_n) was utilized as a structural index for compounds (**1**–**18**). All graphing operations were performed using *Microsoft Office Excel-2003*. The number of carbon atoms in these SWCNT (C_n) seems to be a useful numerical and structural value for characterizing the empty fullerenes. For modeling, both linear (MLR: Multiple Linear Regressions) and nonlinear (ANN: Artificial Neural Network) models were examined in this study. Other indices were examined and the best results and equations for extending the physicochemical and electrochemical data were chosen.

The Rehm–Weller equation estimates the free energy change between an electron donor (D) and an acceptor (A) to be:

$$\Delta G = e[E_D - E_A] - \Delta E^* + \omega_1, \quad (1)$$

where '*e*' is the unit electrical charge, E_D^o and E_A^o are the reduction potentials of the electron donor and acceptor, respectively, ΔE^* is the energy of the singlet or triplet excited state, and ω_1 is the work required to bring the donor and acceptor within the electron transfer (ET) distance. The work term in this expression can be considered to be '0' in as much as there exists an electrostatic complex before the electron transfer [40].

3. Results and discussion

The first reduction processes of Ce@C_{82} and Gd@C_{82} are reversible, and their potentials are very close to those of La@C_{82} and

Y@C_{82} [19]. The first and second oxidations of Gd@C_{82} (+0.09 and +1.08 V) are two-electron processes. On the other hand, the first and second oxidations of Ce@C_{82} are +0.08 and +1.08 V and irreversible. Values were obtained DPV (differential pulse voltammograms) with a pulse amplitude of 50 m, a pulse width of 50 ms, a pulse period of 200 ms, and with a scan rate of 20 mV/s [19]. Interestingly, after one reversible and two irreversible reductions, three other reversible reductions (−1.79, −2.25, and −2.50 V) were observed for Ce@C_{82}. Unlike La@C_{82}, Y@C_{82}, and Gd@C_{82}, the oxidation states of Ce@C_{82} change from 2+ to 6-, not 5-, under the same conditions [19].

It was assumed that all observed reversible redox processes involve a single electron and the results were explained by the following four interpretations [19,41a,b]: (1) The removal of the unpaired electron corresponds to the first oxidation process and the resulting Ln@C_{82}^{+} (Ln = Ce and Gd) should have no radical electrons. (2) Because of the migration of an electron to the HOMO orbital to give the closed-shell species Ln@C_{82} (Ln = Ce and Gd), the first reduction is relatively easy. (3) The low-lying HOMO^{-1} could be responsible for the irreversible formation of Ln@C_{82}^{-}(Ln = Ce and Gd). (4) The ab initio calculations on Ln@C_{82}^{2+} (Ln = Ce and Gd) show that the LUMO and LUMO^{+1} derive from the C_{82} molecular orbitals (MOs), not from the 5*d* and 6*s* atomic orbitals (AOs) of the lanthanum metal [19,41a,b]. Therefore, it was suggested that electrons at least up to the 5-state go to the C_{82} cage rather than to the metal [19].

It was reported that each of the metallofullerene has a remarkably small potential difference between the first oxidation and the first reduction state [19]. This may suggest that the HOMO of M@C_{82}, originally the LUMO^{+} of the C_{82}, is singly occupied (i.e., SOMO) as purposed for Ln@C_{82} [6]. It was found that the ionic radii of Ln^{3+} (lanthanide cations) shows a good linear relationship with the first redox potentials [19]. The ionization potential and electron affinities of M@C_{82} (M = Lanthanides) were obtained by ab initio calculations [19,42]. The first oxidation and reduction processes take place on the SOMO, which has a higher electron density on the cage near the M^{3+} (M = Lanthanides) [19,41a,b,42]. The electrons on the SOMO are bound to the cage stronger when the metal–carbon distance is decreased because the electrostatic interactions between the electrons and the metal increases [19]. Assignment of formal charges to the fullerene cage (that are characterized by the 'charge-per-metal' atom encapsulated) suggests that these metallofullerenes are isoelectronic and have related molecular orbital structures [14]. The potential difference between the oxidation and reduction states in these structures is related to the band gap of the HOMO–LUMO orbitals. It was suggested that these 4*f* electrons do not play an important role in fullerenolanthanide chemistry as seen in organic and inorganic lanthanide chemistry [19,43,44]. The difference between the first oxidation and reduction potentials is very small, probably due to the open-shell electronic structure. The fullerenolanthanides studied in the present work are strong electron donors as well as strong electron acceptors compared to empty fullerenes such as C_{82}. The electronic properties of Ce@C_{82} and Gd@C_{82} are very similar to that of La@C_{82} and Y@C_{82}, although Ce and Gd have 4*f* electrons. This suggests that these 4*f* electrons do not play an important role in fullerenolanthanide chemistry as seen in organic and inorganic lanthanide chemistry [19,31j,k]. Association of the nanostructures, often referred to as molecular clips, with guest molecules depends on weak specific interactions such as hydrogen bonding, ion pairing, dipole–dipole and arene–arene 'π–π' interactions in addition to nonspecific van der Waals forces. The surfaces of complexes [M_x@C_{82}]@[SWCNT(5,5)-armchair-C_nH_{20}] (x = 0, 1; for x = 1: M = Ce & Gd; n = 20–300) have the electro positive and electro negative centers of the plane which can be viewed as enhancement in van der Waals interaction due to availability of greater surface area which will favor strong π–π interaction [31l].

The energy (E_a) is released upon attachment of an electron to an atom or a molecule (A) resulting in the formation of the negative ion A^-, i.e., $A + e^- \rightarrow A^- + E_a$. As in the case of the ionization potential, one can define an adiabatic electron affinity (E_{aa}) and a vertical electron affinity (E_{va}). The adiabatic E_a is equal to the difference between the total energies of a neutral system (A) and the corresponding anion (A^-). The vertical A_X is equal to the difference

Table 1
The values of the relative structural coefficients of [SWCNT(5,5)-armchair-C_nH_{20}] (n = 20–190) **1–18**, C_{82}@[SWCNT(5,5)-armchair-C_nH_{20}] **30–47**, [Ce@C_{82}]@[SWCNT(5,5)-armchair-C_nH_{20}] **48–65** and [Gd@C_{82}]@[SWCNT(5,5)-armchair-C_nH_{20}] **66–83**.[a] Values for [SWCNT(5,5)-armchair-C_nH_{20}] (n = 20–190) **1–18** were calculated and reported at the 6-31G* level (Ref. [28]) and calculated method in the text.

No.	Molecular formula	Point group	Adiabatic electron affinity E_{aa} (eV)	^{Red}E (V)	No.	C_{82}@[SWCNT(5,5)-armchair-C_nH_{20}] **30–47**	No.	[Ce@C_{82}]@[SWCNT (5,5)-armchair-C_nH_{20} **48–65**		No.	[Gd@C_{82}]@[SWCNT (5,5)-armchair-C_nH_{20}] **66–83**	
						$\Delta G_{et(1)}$		$\Delta G_{et(1)}$	$\Delta G_{et(2)}$[b]		$\Delta G_{et(1)}$	$\Delta G_{et(2)}$[b]
1	$C_{20}H_{20}$	D_{5d}	0.34	−0.34	**30**	23.75	**48**	8.99	32.05	**66**	9.22	32.05
2	$C_{30}H_{20}$	D_{5h}	0.89	−0.89	**31**	36.43	**49**	21.67	44.73	**67**	21.90	44.73
3	$C_{40}H_{20}$	D_{5d}	0.67	−0.67	**32**	31.36	**50**	16.60	39.66	**68**	16.83	39.66
4	$C_{50}H_{20}$	D_{5h}	1.14	−1.14	**33**	42.19	**51**	27.44	50.50	**69**	27.67	50.50
5	$C_{60}H_{20}$	D_{5d}	1.56	−1.56	**34**	51.88	**52**	37.12	60.18	**70**	37.35	60.18
6	$C_{70}H_{20}$	D_{5h}	1.34	−1.34	**35**	46.81	**53**	32.05	55.11	**71**	32.28	55.11
7	$C_{80}H_{20}$	D_{5d}	1.61	−1.61	**36**	53.03	**54**	38.27	61.33	**72**	38.51	61.33
8	$C_{90}H_{20}$	D_{5h}	1.98	−1.98	**37**	61.57	**55**	46.81	69.87	**73**	47.04	69.87
9	$C_{100}H_{20}$	D_{5d}	1.71	−1.71	**38**	55.34	**56**	40.58	63.64	**74**	40.81	63.64
10	$C_{110}H_{20}$	D_{5h}	1.91	−1.91	**39**	59.95	**57**	45.20	68.25	**75**	45.42	68.25
11	$C_{120}H_{20}$	D_{5d}	2.24	−2.24	**40**	67.56	**58**	52.80	75.86	**76**	53.03	75.86
12	$C_{130}H_{20}$	D_{5h}	2.06	−2.06	**41**	65.02	**59**	48.65	71.71	**77**	48.88	71.71
13	$C_{140}H_{20}$	D_{5d}	2.13	−2.13	**42**	63.42	**60**	50.27	73.33	**78**	50.50	73.33
14	$C_{150}H_{20}$	D_{5h}	2.43	−2.43	**43**	71.94	**61**	57.18	80.24	**79**	57.41	80.24
15	$C_{160}H_{20}$	D_{5d}	2.35	−2.35	**44**	70.10	**62**	55.34	78.40	**80**	55.57	78.40
16	$C_{170}H_{20}$	D_{5h}	2.23	−2.23	**45**	67.34	**63**	52.57	75.63	**81**	52.80	75.63
17	$C_{180}H_{20}$	D_{5d}	2.53	−2.53	**46**	74.25	**64**	59.49	82.55	**82**	59.72	82.55
18	$C_{190}H_{20}$	D_{5h}	2.45	−2.45	**47**	72.41	**65**	57.65	80.71	**83**	57.88	80.71

[a] The compounds [M_x@C_{82}]@[SWCNT(5,5)-armchair-C_nH_{20}] (x = 0, 1; for x = 1: M = Ce & Gd; n = 20–190) **30–47**, **48–65** and **66–83** were not synthesized or reported. The data of $\Delta G_{et(n)}$ (n = 1 and 2, in kcal mol^{-1}) for supramolecular complexes **30–47**, **48–65** and **66–83** were calculated by the Rehm–Weller equation.

[b] The second oxidation potential of Ce@C_{82} **(b)** and Gd@C_{82} **(c)** are equal ($^{ox}E_2$ = 1.08 V), so the results of the second free energies of electron transfer calculated by Rehm–Weller equation ($\Delta G_{et(2)}$) are equal.

between the total energies of A and the anion A^- in the equilibrium geometry of A [45]. The free energy of this reaction [$\Delta E_s(A \rightarrow A^-)$] corresponds to the absolute redox energy for the above process. The free energy of an electron (e^-) at rest in the gas phase is set to zero [46,47]. It is possible to calculate the redox energy of the reaction ($A + e^- \rightarrow A^- + E_a$) using the thermodynamic equation (see Eq. (2)). In this equation, $\Delta G_s(A)$ and $\Delta G_s(A^-)$ are the solvation energies of molecule A and its anion A^-, respectively, and $\Delta E_g(A \rightarrow A^-)$ is the energy difference between molecule A and its anion (which is defined as the redox energy in the gas phase). On the basis of this thermodynamic cycle, one can obtain $\Delta E_s(A \rightarrow A^-)$, the absolute redox energy, by [46,47]:

$$\Delta E_s(A \rightarrow A^-) = \Delta E_g(A \rightarrow A^-) = \Delta G_s(A) - \Delta G_s(A^-). \quad (2)$$

Thus, by calculating the gas phase energies and solvation energies of molecule A and its anion A^-, one can derive the absolute redox potential (scaled) of molecule A in solution. A scaling coefficient that translates electron affinity to standard redox potentials can thus be extracted [47]. With respect to the interesting results of Ref. [31a], the static, TD-DFT and independently optimized structure were used to calculate the physicochemical and electronic structure of tubular aromatic molecules derived from the metallic (5,5) armchair single-wall carbon nanotubes using the hybrid non-local B3LYP functional [26,48a,b–50].

It is possible to calculate the reduction potential (^{Red}E) of **1–18** using the Gibbs equation ($\Delta G = -n$FE) and the definition of adiabatic electron affinity. In this equation, ΔG is equal to the adiabatic electron affinity (the free energy of electron transfer, ΔG_{et} in J mol^{-1}, 1 eV = 96 471 J mol^{-1}, F = 96 495 coulomb and n = 1). For example, the reduction potentials (^{Red}E) of $C_{20}H_{20}$ and $C_{30}H_{20}$ are equal to −0.34 and −0.89 V. The reduction potentials (^{Red}E) of [SWCNT(5,5)-armchair-C_nH_{20}] (n = 20–190) **1–18** have been calculated and are presented in Table 1. As a rapid result, the amount of ^{Red}E(in Volt) = $-E_{aa}$ (in eV) where E_{aa} is the adiabatic electron affinity. See Table 1.

The values of the relative structural coefficients of the (5,5) armchair SWCNT for $C_{20}H_{20}$ up to $C_{190}H_{20}$ ([SWCNT(5,5)-armchair-C_nH_{20}], **1–18**), the adiabatic electron affinity (E_{aa} in eV) and the reduction potentials (^{Red}E in Volt) of **1–18** are shown in Table 1. The values shown in Table 1 for **1–18** have some mathematical structure. The absolute value of E_{aa} or ^{Red}E increases concomitantly with the number of carbon atoms in **1–18**. From $C_{20}H_{20}$ up to $C_{190}H_{20}$, the point groups alternated between D_{5d} and D_{5h}. By using the Eqs. (5)–(8), the values in Table 1 and Rehm–Weller equation the results are extended in Table 2 for compounds **19–29**.

Eqs. (3) and (4) show the relationship between the values of the number of carbon atoms (n) of these [SWCNT(5,5)-armchair] versus the adiabatic electron affinity (E_{aa} in eV) and the reduction potential (^{Red}E in Volt) of [SWCNT(5,5)-armchair-C_nH_{20}] (n = 20–190) **1–18**, respectively. Eq. (5), similar to Eq. (4), shows the *Nieperian* logarithmic behavior of the relationship. The R-squared value (R^2) for the graphs was found to be 0.9461.

$$E_{aa} = 22.417\ \mathrm{Ln}(n) - 58.553, \quad (3)$$

$$^{Red}E = 0.9721\ \mathrm{Ln}(n) - 2.6088. \quad (4)$$

Using these equations, it is possible to achieve a good approximation for extending the determination of the adiabatic electron affinity (E_{aa}) and the reduction potential (^{Red}E) for the other [SWCNT(5,5)-armchair-C_nH_{20}] (n = 200–300) **19–29**.

Table 1 also shows the values of the relative structural coefficients, the adiabatic electron affinity (E_{aa} in eV) and the reduction potential (^{Red}E in Volt) of [SWCNT(5,5)-armchair-C_nH_{20}] (n = 20–190) **1–18** and fullerene C_{82}, the endohedral-metallofullerenes Ce@C_{82} and Gd@C_{82} as [M_x@C_{82}]@[SWCNT(5,5)-armchair-C_nH_{20}]

Table 2
The values of the relative structural coefficients of [SWCNT(5,5)-armchair-C_nH_{20}] (n = 20–190) **19–29**, C_{82}@[SWCNT(5,5)-armchair-C_nH_{20}] **84–94**, [Ce@C_{82}]@[SWCNT(5,5)-armchair-C_nH_{20}] **95–105** and [Gd@C_{82}]@[SWCNT(5,5)-armchair-C_nH_{20}] **106–116**.[a]

No.	Molecular formula	Point group	Adiabatic electron affinity E_{aa} (eV)	^{Red}E (V)	No.	C_{82}@[SWCNT (5,5)-armchair-C_nH_{20}] **84–94**		No.	[Ce@C_{82}]@[SWCNT(5,5)-armchair-C_nH_{20}] **95–105**			No.	[Gd@C_{82}]@[SWCNT(5,5)-armchair-C_nH_{20}] **106–116**			
						$\Delta G_{et(1)}$ (kcal mol^{-1})			$\Delta G_{et(1)}$ (kcal mol^{-1})		$\Delta G_{et(2)}$ (kcal mol^{-1})		$\Delta G_{et(1)}$ (kcal mol^{-1})		$\Delta G_{et(2)}$ (kcal mol^{-1})	
						Eq. (5)	Rehm–Weller		Eq. (6)	Rehm–Weller	Eq. (8)	Rehm–Weller	Eq. (7)	Rehm–Weller	Eq. (8)	Rehm–Weller
19	$C_{200}H_{20}$	D_{5d}	2.49	−2.49	**84**	74.50	73.33	**95**	59.75	58.57	82.81	81.63	**106**	59.98	58.80	82.81	81.63
20	$C_{210}H_{20}$	D_{5h}	2.53	−2.53	**85**	75.59	74.25	**96**	60.85	59.49	83.90	82.55	**107**	61.08	59.72	83.90	82.55
21	$C_{220}H_{20}$	D_{5d}	2.57	−2.57	**86**	76.63	75.17	**97**	61.89	60.42	84.95	83.48	**108**	62.12	60.65	84.95	83.48
22	$C_{230}H_{20}$	D_{5h}	2.60	−2.60	**87**	77.63	75.87	**98**	62.89	61.11	85.94	84.17	**109**	63.11	61.34	85.94	84.17
23	$C_{240}H_{20}$	D_{5d}	2.64	−2.64	**88**	78.58	76.79	**99**	63.84	62.03	86.90	85.09	**110**	64.07	62.26	86.90	85.09
24	$C_{250}H_{20}$	D_{5h}	2.67	−2.67	**89**	79.50	77.48	**100**	64.76	62.72	87.81	85.78	**111**	64.98	62.95	87.81	85.78
25	$C_{260}H_{20}$	D_{5d}	2.71	−2.71	**90**	80.37	78.40	**101**	65.64	63.65	88.69	86.71	**112**	65.86	63.88	88.69	86.71
26	$C_{270}H_{20}$	D_{5h}	2.74	−2.74	**91**	81.22	79.10	**102**	66.48	64.34	88.54	87.40	**113**	66.71	64.57	88.54	87.40
27	$C_{280}H_{20}$	D_{5d}	2.77	−2.77	**92**	82.03	79.79	**103**	67.30	65.03	90.35	88.09	**114**	67.52	65.26	90.35	88.09
28	$C_{290}H_{20}$	D_{5h}	2.80	−2.80	**93**	82.82	80.48	**104**	68.08	65.72	91.14	88.78	**115**	68.31	65.95	91.14	88.78
29	$C_{300}H_{20}$	D_{5d}	2.83	−2.83	**94**	83.58	81.17	**105**	68.84	66.41	91.90	89.47	**116**	69.07	66.64	91.90	89.47

[a] The complexes **84–94**, **95–105** and **106–116** were not synthesized and nor reported previously.

(x = 0, 1; for x = 1: M = Ce & Gd; n = 20–190) **30–47**, **48–65** and **66–83**, by the Rehm–Weller equation.

Fig. 2 shows the relationship between the number of carbon atoms (n) in the [SWCNT(5,5)-armchair] and the first free energy of electron transfer ($\Delta G_{et(1)}$, kcal mol^{-1}) of C_{82}@[SWCNT(5,5)-armchair-C_nH_{20}] **30–47** as presented in Table 1. Eq. (5) applies to Fig. 2 and shows the *Nieperian* logarithmic behavior of the relationship. Using this equation, it is possible to achieve a good approximation for extending the first free energy of electron transfer ($\Delta G_{et(1)}$) for the other structures of C_{82}@[SWCNT(5,5)-armchair-C_nH_{20}] **84–94** (n = 200–300). The R-squared value (R^2) for this graph was found to be 0.9448.

$$\Delta G_{et(1)} = 22.400\ \mathrm{Ln}(n) - 44.184. \quad (5)$$

The predicted values of $\Delta G_{et(1)}$ for C_{82}@[SWCNT(5,5)-armchair-C_nH_{20}] **84–94** (n = 200–300) were calculated using Eq. (5) (see Table 2).

Fig. 2 shows the relationship between the number of carbon atoms (n) in the [SWCNT(5,5)-armchair] versus the first free energy of electron transfer ($\Delta G_{et(1)}$, kcal mol^{-1}) of [Ce@C_{82}]@[SWCNT(5,5)-armchair-C_nH_{20}] **48–65** as presented in Table 1. Eq. (6) applies to Fig. 2 and shows the *Nieperian* logarithmic behavior of the relationship. Using this equation, it is possible to achieve a good approximation for extending the first free energy of electron transfer ($\Delta G_{et(1)}$) for the other [Ce@C_{82}]@[SWCNT(5,5)-armchair-C_nH_{20}] **95–105** (n = 200–300). The R-squared value (R^2) for this graph was found to be 0.9462.

$$\Delta G_{et(1)} = 22.416\ \mathrm{Ln}(n) - 59.011. \quad (6)$$

The predicted values of $\Delta G_{et(1)}$ for [Ce@C_{82}]@[SWCNT(5,5)-armchair-C_nH_{20}] **95–105** (n = 200–300) were calculated using Eq. (6) (see Table 2).

Eq. (7) shows the relationship between the number of carbon atoms (n) of these SWCN(5,5)-Armchair versus the first free energy of electron transfer ($\Delta G_{et(1)}$, kcal mol^{-1}) of [Gd@C_{82}]@[SWCNT(5,5)-armchair-C_nH_{20}] **66–83**. Eq. (7), similar to Eqs. (5) and (6), shows the *Nieperian* logarithmic behavior of the relationship. The R-squared value (R^2) for this graph was found to be 0.9462.

$$\Delta G_{et(1)} = 22.415\ \mathrm{Ln}(n) - 58.779. \quad (7)$$

Using this equation, it is possible to achieve a good approximation for extending the determination of the first free energy of electron transfer ($\Delta G_{et(1)}$) for the other [Gd@C_{82}]@[SWCNT(5,5)-armchair-C_nH_{20}] (n = 200–300) **106–116**.

The relationship between the number of carbon atoms (n) of [SWCNT(5,5)-armchair-C_nH_{20}] (n = 20–190) **1–18** versus the second free energy of electron transfer ($\Delta G_{et(2)}$, kcal mol^{-1}) of [Ce@C_{82}]@[SWCNT(5,5)-armchair-C_nH_{20}] **48–65** and [Gd@C_{82}]@[SWCNT(5,5)-armchair-C_nH_{20}] **66–83** are shown in Eq. (8). Eq. (8) also exhibits *Nieperian* logarithmic behavior for $\Delta G_{et(2)}$ of the both groups of [M@C_{82}]@[SWCNT(5,5)-armchair-C_nH_{20}] (M = Ce and Gd, n = 20–190). The R-squared value (R^2) for this graph was found to be 0.9462.

$$\Delta G_{et(2)} = 22.415\ \mathrm{Ln}(n) - 35.950. \quad (8)$$

Using this equation, it is possible to extend the calculation of the second free energy of electron transfer ($\Delta G_{et(2)}$ in kcal mol^{-1}) for some of the other supramolecular structures of [Ce@C_{82}]@[SWCNT(5,5)-armchair-C_nH_{20}] **48–65** and [Gd@C_{82}]@[SWCNT(5,5)-armchair-C_nH_{20}] **66–83**.

There is a strong linear relationship between the adiabatic electron affinity (E_{aa} in eV) and the reduction potential (^{Red}E in Volt) of [SWCNT(5,5)-armchair-C_nH_{20}] (n = 20–190) **1–18** versus the first and second free energy of electron transfer ($\Delta G_{et(n)}$, n = 1, 2 in kcal mol^{-1}) of C_{82}@[SWCNT(5,5)-armchair-C_nH_{20}] **30–47** (first electron transfer energy ($\Delta G_{et(1)}$ on the basis of first oxidation potential of C_{82}), [Ce@C_{82}]@[SWCNT(5,5)-armchair-C_nH_{20}] **48–65** and [Gd@C_{82}]@[SWCNT(5,5)-armchair-C_nH_{20}] **66–83**.

In light of the good linear correlations between $\Delta G_{et(n)}$ (n = 1, 2), E_{aa} and ^{Red}E of **1–18** with **30–47**, **48–65** and **66–83**, respectively, it is possible to use the values of E_{aa} and ^{Red}E to calculate the free energies of electron transfer (ΔG_{et} in kcal mol^{-1}) of [M_x@C_{82}]@[SWCNT(5,5)-armchair-C_nH_{20}] (x = 0, 1; for x = 1: M = Ce & Gd; n = 200–300 **84–94**, **95–105** and **106–116**. The electron affinity and the reduction potential are in fact the same magnitude with the sign reversed, whereas the free energy of electron transfer is calculated with the Rehm–Weller equation, which can be straightforwardly proven to be linearly dependent on the electron affinity of the compounds studied here. In Table 2, the values of the free energies of electron transfer obtained for compounds **84–94**, **95–105** and **106–116** from the Eqs. (5)–(8) and those obtained with the Rehm–Weller equation are compared.

The values of the number of carbon atoms (n), E_{aa}, ^{Red}E and $\Delta G_{et(n)}$ (n = 1, 2) of [SWCNT(5,5)-armchair-C_nH_{20}] (n = 200–300) **19–29** and their complexes with C_{82} (**a**), Ce@C_{82} (**b**) and Gd@C_{82} (**c**), ([M_x@C_{82}]@[SWCNT(5,5)-armchair-C_nH_{20}] (x = 0, 1; for x = 1: M = Ce & Gd; n = 200–300) **84–94**, **95–105** and **106–116**) are shown in Table 2. The results of the reduction potentials (^{Red}E in Volt) were extended for $C_{200}H_{20}$ up to $C_{300}H_{20}$ ([SWCNT(5,5)-armchair-C_nH_{20}], **19–29**). The calculated results for ^{Red}E, as well as the free energies of electron transfer ($\Delta G_{et(n)}$, n = 1, 2, in kcal mol^{-1}) according to the Rehm–Weller equation between C_{82} (**a**), Ce@C_{82} (**b**) and Gd@C_{82} (**c**) with [SWCNT(5,5)-armchair-C_nH_{20}], **19–29** in the structures [M_x@C_{82}]@[SWCNT(5,5)-armchair-C_nH_{20}] (x = 0, 1; for x = 1: M = Ce & Gd; n = 200–300 **84–94**, **95–105** and **106–116** are presented in Table 2.

In Figs. 2 and 3, the periodicity of the points plotted appears to be 3, which is quite common among benzenoids. By using Eq. (1) (Rehm–Weller equation) and Eqs. (2)–(8), the values of E_{aa}, ^{Red}E and $\Delta G_{et(n)}$ (n = 1, 2) were calculated for **19–29**, **84–94**, **95–105** and **106–116**. The values of the number of carbon atoms (n) show a good relationship with the values of the adiabatic electron affinity (E_{aa} in eV), the values of the reduction potential (^{Red}E in Volt) of [SWCNT(5,5)-armchair-C_nH_{20}] (n = 20–190) **1–18** and **19–29** and the free energy of electron transfer (ΔG_{et} in kcal mol^{-1}) in the [M_x@C_{82}]@[SWCNT(5,5)-armchair-C_nH_{20}] (x = 0, 1; for x = 1:

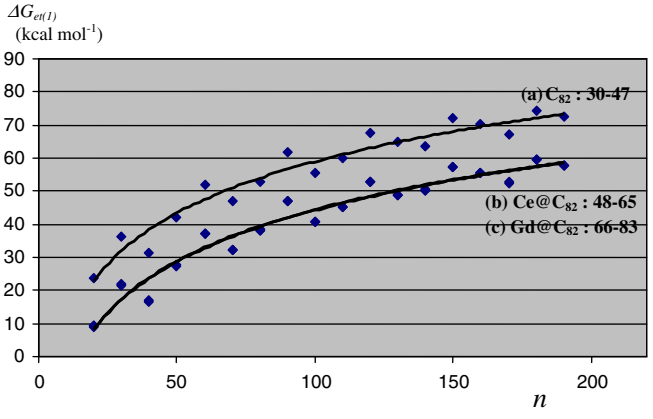

Fig. 2. The relationship between the number of carbon atoms 'n' and the first free energy of electron transfer ($\Delta G_{et(1)}$, kcal mol^{-1}) of C_{82}@[SWCNT(5,5)-armchair-C_nH_{20}] **30–47** (for C_{82} (**a**)), [Ce@C_{82}]@[SWCNT(5,5)-armchair-C_nH_{20}] **48–65** (for Ce@C_{82} (**b**)) and [Gd@C_{82}]@[SWCNT(5,5)-armchair-C_nH_{20}] **66–83** (for Gd@C_{82} (**c**)). The first oxidation potential of Ce@C_{82} (**b**) and Gd@C_{82} (**c**) are near ($^{ox}E_1$ = 0.08 and 0.09 V, respectively), so the curve of the results of the second free energies of electron transfer calculated by Rehm–Weller equation ($\Delta G_{et(1)}$) are approximately pasted.

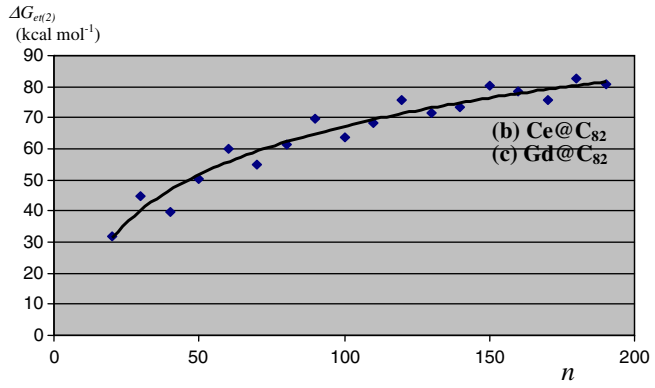

Fig. 3. The relationship between the number of carbon atoms '*n*' and the second free energy of electron transfer ($\Delta G_{et(2)}$, kcal mol^{-1}) of [Ce@C_{82}]@[SWCNT(5,5)-armchair-C_nH_{20}] **48–65** (for Ce@C_{82} **(b)**) and [Gd@C_{82}]@[SWCNT(5,5)-armchair-C_nH_{20}] **66–83** (for Gd@C_{82} **(c)**). The second oxidation potential of Ce@C_{82} **(b)** and Gd@C_{82} **(c)** are equal ($^{ox}E_2$ = 1.08 V), so the results of the second free energies of electron transfer calculated by Rehm–Weller equation ($\Delta G_{et(2)}$) are equal.

M = Ce & Gd; *n* = 20–300) **30–47**, **48–65**, **66–83**, **84–94**, **95–105** and **106–116**. With the above equations, it is possible to calculate the adiabatic electron affinity (E_{aa} in eV), the values of the reduction potential (^{Red}E in Volt) in **1–18** and **19–29** and the first and second free energies of electron transfer (ΔG_{et} in kcal mol^{-1}) in the **30–47**, **48–65**, **66–83**, **84–94**, **95–105** and **106–116** with good approximation. The armchair single-wall nanotubes [SWCNT(5,5)-armchair-C_nH_{20}] (*n* = 20–300) **1–18**, **19–29** and their supramolecular complexes with C_{82} (**a**), Ce@C_{82} (**b**) and Gd@C_{82} (**c**), i.e. [M_x@C_{82}]@[SWCNT(5,5)-armchair-C_nH_{20}] (x = 0, 1; for x = 1: M = Ce & Gd; n = 20–300) **30–47**, **48–65**, **66–83**, **84–94**, **95–105** and **106–116** were neither synthesized nor reported before.

4. Conclusions

Nano-scale materials have important applications in many areas of science such as in the creation of computers, microchips, sensors, actuators and machines. Nanoscale structures of carbon display an attractive variation of structural characteristics, and many useful forms have been synthesized and identified. Three of these structures are the SW carbon nanotubes (SWCNT), fullerenes (C_n) and endohedral-metallofullerenes (M@C_n). Graph theory applications have provided different mathematical methods for finding the relationships between several numerical properties of these materials. In this study, the structural relationships between the number of carbon atoms (n) index and the adiabatic electron affinity (E_{aa} in eV), the values of the reduction potential (^{Red}E in Volt) of [SWCNT(5,5)-armchair-C_nH_{20}] (*n* = 20–190) **1–18** and **19–29** and the free energies of electron transfer ($\Delta G_{et(n)}$, n = 1, 2 in kcal mol^{-1}) in the [M_x@C_{82}]@[SWCNT(5,5)-armchair-C_nH_{20}] (x = 0, 1; for x = 1: M = Ce & Gd; *n* = 20–300) **30–47**, **48–65**, **66–83**, **84–94**, **95–105** and **106–116** were demonstrated. The number of carbon atoms show a strong correlation with the values of E_{aa} and ^{Red}E in the (5,5) armchair SWCNT **1–18** and **19–29** as important factors in characterizing these materials. The values of ΔG_{et} were calculated using the Rehm–Weller equation for **30–47**, **48–65**, **66–83**, **84–94**, **95–105** and **106–116**. Using this model and the associated equations, it is possible to calculate in a simple manner and with good approximation the E_{aa}, ^{Red}E and $\Delta G_{et(n)}$ (n = 1, 2 in kcal mol^{-1}) of this family of compounds **19–29** and the complexes with C_{82} (**a**), Ce@C_{82} (**b**) and Gd@C_{82} (**c**), **30–47**, **48–65**, **66–83**, **84–94**, **95–105** and **106–116**. The model can be used to study structural properties, the electron affinity, the reduction potential and the first and second free energies of electron transfer properties of these types of nanotubes (5,5), armchair SWCNTs and their supramolecular structures [M_x@C_{82}]@[SWCNT(5,5)-armchair-C_nH_{20}] (x = 0, 1; for x = 1: M = Ce and Gd).

Acknowledgments

The author gratefully acknowledges his colleagues in the Chemistry Department of The University of Queensland-Australia for their useful suggestions.

References

[1] K. Kikuchi et al., Nature 357 (1992) 142.
[2] W. Krätschmer, L.D. Lamb, K. Fostiropoulos, D.R. Huffman, Nature 347 (1990) 354.
[3] F. Diederich et al., Science 252 (5005) (1991) 548.
[4] R. Ettl, I. Chao, F. Diederich, R.L. Whetten, Nature 353 (6340) (1991) 149.
[5] K. Kikuchi et al., Chem. Lett. (1991) 1607.
[6] K. Kikuchi et al., Chem. Phys. Lett. 188 (1991) 177.
[7] H.W. Kroto, J. Heath, S.C. O'Brien, R.F. Curl, R.E. Smalley, Nature 318 (1985) 162.
[8] D.E. Manolopoulos, P.W. Fowler, Chem. Phys. Lett. 187 (1991) 1.
[9] D.E. Manolopoulos, P.W. Fowler, J. Chem. Phys. 96 (1992) 7603.
[10] F. Diederich, R.L. Whetten, C. Thilgen, R. Ettl, I. Chao, M.M. Alvarez, Science 254 (1991) 1768.
[11] X.Q. Wang, C.Z. Wang, B.L. Zhang, K.M. Ho, Chem. Phys. Lett. 217 (1994) 199.
[12] G. Sun, M. Kertesz, J. Phys. Chem. A 105 (22) (2001) 5468.
[13] (a) The website of L. Dunsch, IFW-Dresden-Germany, <http://www.ifw-dresden.de/institutes/iff/research/Carbon/fullerenes/introduction>; (b) <http://en.wikipedia.org/wiki/Fullerene>.
[14] M.R. Anderson, H.C. Dorn, S.A. Stevenson, Carbon 38 (2000) 1663. and the literature cited therein.
[15] J.H. Weaver, Y. Chai, G.H. Kroll, C. Jin, T.R. Ohno, R.E. Haufler, et al., Chem. Phys. Lett. 190 (5) (1992) 460.
[16] R.E. Smalley, in: G.S. Hamond, V.J. Kuck (Eds.), Fullerenes, American Chemical Society, Washington, DC, 1992, p. 141.
[17] C.S. Yannoni, M. Hoinkis, M.S. De Vries, D.S. Bethune, J.R. Salem, M.S. Crowder, et al., Science 256 (5060) (1992) 1191.
[18] R.S. Ruoff, K.M. Kadish, P. Boulas, E.C.M. Chen, J. Phys. Chem. 99 (21) (1995) 8843.
[19] T. Suzuki, K. Kikuchi, F. Oguri, Y. Nakao, S. Suzuki, Y. Achiba, et al., Tetrahedron 52 (14) (1996) 4973. and the literature cited therein.
[20] D.S. Bethune, R.D. Johnson, J.R. Salem, M.S. De Vries, C.S. Yannoni, Nature 366 (1993) 123.
[21] Y. Chai, T. Guo, C. Jin, R.E. Haufler, L.P.F. Chibante, J. Fure, et al., J. Phys. Chem. 95 (20) (1991) 7564.
[22] R.D. Johnson, M.S. De Vries, J. Salem, D.S. Bethune, C.S. Yannoni, Nature 355 (1992) 239.
[23] D.R. Lide (Ed.), Handbook of Chemistry and Physics, 75th Edn., CRC Press, Boca Raton, 1994, p. 4.
[24] R.D. Shannon, Acta Crystallogr., Sect. A 32 (1976) 751.
[25] S. Nagase, K.J. Kobayashi, J. Chem. Soc., Chem. Commun. 4 (1994) 1837.
[26] Z. Zhou, M. Steigerwald, M. Hybertsen, L. Brus, R.A. Friesner, J. Am. Chem. Soc. 126 (11) (2004) 3597. and the literature cited therein.
[27] D. Srivastava, M. Menon, K. Cho, Comput. Sci. Eng. 3 (2001) 42. and the literature cited therein.
[28] O. Lourie, D.M. Cox, H.D. Wagner, Phys. Rev. Lett. 81 (1998) 1638.
[29] S. Nagase, K. Kobayashi, J. Chem. Soc. Chem. Commun. 16 (1994) 1837.
[30] (a) D. Dubois, K.M. Kadish, S. Flanagan, L.J. Wilson, J. Am. Chem. Soc. 113 (20) (1991) 7773;
(b) Q. Xie, E. Pérez-Cordero, L. Echegoyen, J. Am. Chem. Soc. 114 (10) (1992) 3978;
(c) Y. Ohsawa, T. Saji, J. Chem. Soc. Chem. Commun. 10 (1992) 781;
(d) Q. Li, F. Wudl, C. Thilgen, R.L. Whetten, F. Diederich, J. Am. Chem. Soc. 114 (10) (1991) 3994.
[31] (a) J.S. Arellano, L.M. Molina, A. Rubio, M.J. Lopez, J.A. Alonso, J. Chem. Phys. 117 (5) (2002) 2281;
(b) D. Srivastava, S. Barnard, Molecular dynamics simulation of large scale carbon nanotubes on a shared memory architecture, in: Proc. IEEE Supercomputing '97, IEEE Computer Soc. Press, Los Alamitos, CA, 1997;
(c) B.I. Yakobson, C.J. Brabec, J. Bernholc, Phys. Rev. Lett. 76 (1996) 2511;
(d) D. Srivastava, M. Menon, K. Cho, Phys. Rev. Lett. 83 (1999) 2973;
(e) B.I. Yakobson, P. Avouris, Mechanical Properties of Carbon Nanotubes, Springer-Verlag, Berlin, 2001. p. 293;
(f) M.S. Dresselhaus, G. Dresselhaus, P.C. Eklund, Science of Fullerenes and Carbon Nanotubes, Academic Press, New York, 1996;
(g) P. Avouris, Acc. Chem. Res. 35 (12) (2002) 1026;
(h) M.S. Dresselhaus, G. Dresselhaus, P. Avouris (Eds.), Carbon Nanotubes: Synthesis, Structure Properties and Applications, Springer-Verlag, Berlin, 2001;
(i) Special issue on carbon nanotubes, Physics World 13 (6) (2000).;
(j) P.G. Collins, P. Avouris, Sci. Am. 283 (2000) 38;

(k) M.S. Dresselhaus, G. Dresselhaus, R. Saito, Phys. Rev. B 45 (11) (1992) 6234;
(l) J.W. Mintmire, B.I. Dunlap, C.T. White, Phys. Rev. Lett. 68 (1992) 631;
(m) R. Barnett, E. Demler, E. Kaxiras, Solid State Commun. 135 (5) (2005) 335;
(n) A. Sygula, F.R. Fronczek, R. Sygula, P.W. Rabideau, M.M. Olmstead, J. Am. Chem. Soc. 129 (2007) 3842.
[32] (a) M.V. Diudea, Fulle. Nanot. Carb. Nanost. (FNCN) 10 (4) (2002) 273;
(b) M.V. Diudea, J. Chem. Inf. Model. 45 (2005) 1002;
(c) M.V. Diudea, Polyhex tori originating in square tiled tori, in: M.V. Diudea (Ed.), Nanostructures, Novel Architecture, NOVA 2005, pp. 111–126.
[33] D. Srivastava, S.N. Atluri, CMES 3 (5) (2002) 531.
[34] L. Kavan, L. Dunsch, H. Kataura, Carbon 42 (5–6) (2004) 1011.
[35] B.S. Sherigara, W. Kutner, F. D'Souza, Electroanalysis 15 (9) (2003) 753.
[36] S. Bandow, M. Takizawa, H. Kato, T. Okazaki, H. Shinohara, S. Iijima, Chem. Phys. Lett. 347 (1–3) (2001) 23.
[37] (a) A.A. Taherpour, Chem. Phys. Lett. 469 (2009) 135;
(b) A.A. Taherpour, Fulle. Nanot. Carb. Nanost. (FNCN) 16 (3) (2008) 196;
(c) A.A. Taherpour, Fulle. Nanot. Carb. Nanost. (FNCN) 15 (4) (2007) 279;
(d) A.A. Taherpour, F. Shafiei, J. Mol. Struct. Theochem. 726 (1–3) (2005) 183;
(e) A.A. Taherpour, J. Phys. Chem. C 113 (2009) 5402.
[38] (a) P.J. Hansen, P. Jurs, J. Chem. Educ. 65 (7) (1988) 574. and the literature cited therein;
(b) H. Hosoya, Bull. Chem. Soc. Jpn. 44 (1971) 2332;
(c) M. Randić, Acta Chim. Slov. 45 (3) (1998) 239;
(d) G. Rücker, C. Rücker, J. Chem. Inf. Comput. Sci. 39 (5) (1999) 788;
(e) H. Wiener, J. Am. Chem. Soc. 69 (1) (1947) 17.
[39] (a) Y.P. Du, Y.Z. Liang, B.Y. Li, C.J. Xu, J. Chem. Inf. Comput. Sci. 42 (5) (2002) 993;
(b) M. Randić, J. Am. Chem. Soc. 97 (23) (1975) 6609;
(c) S.D. Bolboaca, L. Jantschi, Int. J. Mol. Sci. 8 (4) (2007) 335;
(d) Z. Slanina, F. Uhlik, S.L. Lee, E. Osawa, Match Commun. Math. Comput. Chem. 44 (2001) 335.
[40] D. Rehm, A. Weller, Isr. J. Chem. 8 (1970) 259.
[41] (a) S. Nagase, K. Kobayashi, T. Kato, Y. Achiba, Chem. Phys. Lett. 201 (5–6) (1993) 475;
(b) S. Nagase, K. Kobayashi, Chem. Phys. Lett. 214 (1) (1993) 57.
[42] K. Laasonen, K. Laasonen, W. Andreoni, M. Parrinello, Science 258 (5090) (1992) 1916.
[43] T.J. Marks, R.D. Ernst, in: G. Wilkinson, F.G.A. Stone, E.W. Abel (Eds.), Comprehensive Organometallic Chemistry, Pergamon Press, Oxford, 1982 (Chapter 21).
[44] F.A. Cotton, G. Wilkinson, Advanced Inorganic Chemistry, John Wiley & Sons, New York, 1988 (Chapter 20).
[45] Cite of: International Union of pure and applied chemistry.htm, Pure Appl. Chem. (IUPAC), 71 (10) (1999) 1919–1981.
[46] L.Y. Zhang, R.A. Friesner, J. Phys. Chem. 99 (44) (1995) 16479.
[47] I.A. Topol, C. McGrath, E. Chertova, C. Dasenbrock, W.R. Lacourse, M.A. Eissenstat, et al., Protein Sci. 10 (7) (2001) 1434.
[48] (a) A.D. Becke, J. Chem. Phys. 98 (7) (1993) 5648;
(b) K. Raghavachari, Theor. Chem. Acc. 103 (2001) 361.
[49] J. Muscat, A. Wander, N.M. Harrison, Chem. Phys. Lett. 342 (3–4) (2001) 397.
[50] J.K. Perry, J. Tahir-Kheli, W.A. Goddard, Phys. Rev. B 65 (14) (2002) 144501.